Duration of Individual Relativistic Electron Microbursts: A Probe Into Their Scattering Mechanism

M. Shumko[1], L.W. Blum[2], and A.B. Crew[3]

[1]NASA's Goddard Space Flight Center, Greenbelt, Maryland
[2]University of Colorado Boulder, Boulder, Colorado
[3]Johns Hopkins University Applied Physics Laboratory, Laurel, Maryland

Key Points:

- We identified relativistic microbursts observed by the SAMPEX satellite and quantified their duration
- Microburst duration roughly doubles between the midnight and noon magnetic local time regions
- Whistler-mode chorus rising tone element duration has a similar trend

Corresponding author: M. Shumko, `msshumko@gmail.com`

Abstract

In this study we used the Solar Anomalous and Magnetospheric Particle Explorer to identify relativistic, > 1 MeV, microbursts and we quantified their duration. We found that the microburst duration is shortest near midnight magnetic local times and is longest, by a factor of two, near noon magnetic local times.

Plain Language Summary

Microbursts are a naturally occurring form of electron precipitation from the near-Earth space into the atmosphere. They are characterized by their short duration, typically defined to be less than a second, or sometimes as 100 milliseconds... Microburst impact on the atmosphere includes the degradation of Mesospheric Ozone through the production of Odd Nitrogen and Odd Hydrogen molecules... We don't know the details on how microburst electrons are scattered, but there is evidence that they are scattered by whistler-mode chorus rising tone elements... Talk about duration and how it is a probe into the scattering physics.

1 Introduction

Outline

1. Introduce particle accelerating/scattering mechanism... dual role of chorus waves.
2. One manifestation of electron-chorus scattering are electron microbursts.
3. Briefly describe microbursts and their properties.
4. Mention the chorus-microburst link, but it is currently unknown the physics of how electrons get scattered. Two approaches are quasi-linear diffusion and non-linear scatterring.
5. Talk about microburst-chorus rising tone element duration and how they are similar. Mention the prior microburst width studies.
6. The microburst width has not been explored as a function of geomagnetic indices or location.
7. The trends in microburst width (duration) can be a probe into the conditions necessary to scatter microburst electrons.

2 Instrumentation

Outline

1. Describe SAMPEX
2. Describe HILT
3. Describe the 20 ms data used in this study (State4, 20 ms, avoided spin times). Data duration.

In this study we used data taken by the Solar Anomalous Magnetospheric Particle Explorer (SAMPEX) satellite

3 Methodology

Outline

1. The methodology consists of two main steps: identify microbursts and estimate their duration.

2. We identified microbursts using the Burst parameter. Mention the bias and how we addressed it.
3. Discuss biases to short width, low counts. Douma 2019 showed that the microburst fluxes are roughly uniform in MLT (could this comparison be invalid since Douma also used the burst parameter?)
4. Ref Fig 1 microbursts.
5. Estimate microburst width using two methods:
6. The prominence width method (cite my other paper).
7. Gaussian + trend fit. Trend is important to approximate the drifting electrons in the DLC. automating fits is difficult so we helped out: the initial parameter guesses were provided from the prominence method, and the quality of fit checked with the r^2 and adj r^2. Provide the definition of r^2 used here and state the goodness of fit threshold we used.
8. Ref Fig 1 microbursts + fits. Mention the benefit of the linear trend, and screening out of multiple, superposed microbursts, by r2.

To estimate the microburst duration we first identified microbursts and then we fit them with a Gaussian function.

3.1 Microburst Identification

We identified microbursts using the burst parameter defined by O'Brien et al. (2003) and used in numerous other microburst studies with SAMPEX (e.g. Douma et al., 2017). Assuming Poisson probability for the observed electron counts, the burst parameter is the number of standard deviations of a foreground signal above the background. It is generally defined as

$$bp = \frac{N - A}{\sqrt{A+1}} \tag{1}$$

Find a better variable than bp. This is not British Petroleum where N is the number of foreground electron counts (microburst or otherwise), and A is the centered running average counts representing the background. The 1 in the denominator prevents a division by 0 error. In O'Brien et al. (2003), and in the results in this study, N was summed over 0.1 seconds and is called N_{100}, while A parameter was summed over 0.5 seconds and is called A_{500}. Henceforth we will specify the time window with the subscript for N and A. With A_{500} and N_{100}, we detected a total of 256,764 microbursts over the 13 year period from 1997 to 2012. Four examples of microbursts are shown in Fig. 1 by the solid black curves.

The choice of A determines the sensitivity of the burst parameter to microbursts of various durations (widths). This sensitivity is best illustrated with an example. Given a 1-second wide microburst, if we use A_{500}, the centered average background at the microburst time is scewed higher towards the microburst peak. The average is dominated heavily by the microburst counts. On the other hand, if we use A_{1000}, the background will not be elevated as much because more true background counts will be included in the average. Therefore, bp will be relatively larger for A_{1000} than A_{500}. This sensitivity manifests itself as a bias towards narrower microbursts that we will address later in this study.

3.2 Microburst Duration

We estimated the microburst duration using two methods: the duration at half of the microburst's topographic prominence and Guassian fits.

$$c(t|A, t_0, \sigma, c_0, c_1) = Ae^{-\frac{(t-t_0)^2}{2\sigma^2}} + c_0 + c_1 t \tag{2}$$

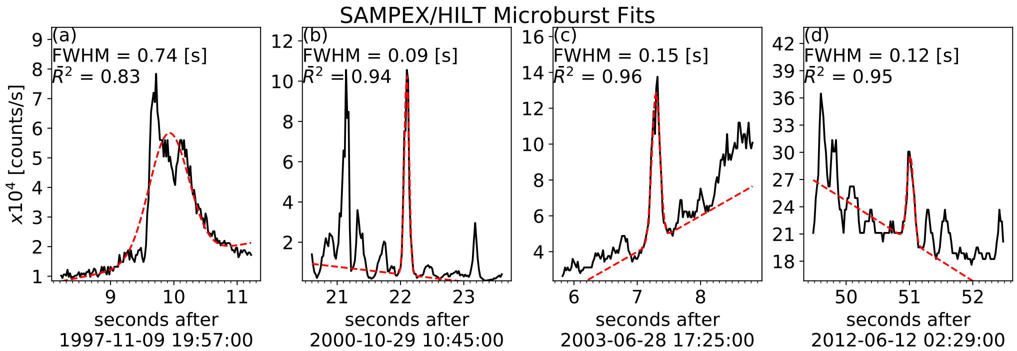

Figure 1. Example $>$ 1 MeV microbursts shown by the black lines, and the fits shown by the dashed red lines. The fit full width at half maximum (FWHM) and the $\bar{R}^2$ goodness of fit metric is annotated in each panel. The major time ticks are at every second, while the minor ticks are at every 100 milliseconds.

where A, t_0, and σ are the Gaussian amplitude, center time, and standard deviation; while the c_0 and c_1 are the background count intercept and slope. The fit was applied over the the following duration, and the initial parameter guess was provided by X. The optimal fit parameters were found using Python's `scipy.curve_fit()` function.

To evaluate the fit, the R^2 goodness of fit metric was used. R^2 is defined as

$$R^2 = 1 - \frac{SS_{res}}{SS_{total}} = 1 - \frac{\sum (c_i - f_i)^2}{\sum (c_i - \bar{c})^2} \tag{3}$$

where SS_{res} is the sum of squares of the residuals between the observed counts c_i and the fit counts f_i for each time stamp, and SS_{total} is the sum of squares between c_i and the mean counts $\bar{c}$.

One interpretation of R^2 is: fractionally how much better the model fit explains the variance in the data, compared to a null hypothesis horizontal line fit at $\bar{c}$. When $R^2 = 1$, the modeled fit perfectly describes the variance in the data, and R^2 can be arbitrarily negative for poor fits (a fit can be much worse than the mean).

To account for overfitting that results from the variable number of data points used for each fit, the adjusted R^2, $\bar{R}^2$ was used. It is defined as

$$\bar{R}^2 = 1 - (1 - R^2)\frac{n-1}{n-p-1} \tag{4}$$

where n is the number of data points fit, and p is the number of parameters. Intuitively, $n-1$ is the number of degrees of freedom for the null hypothesis, and $n-p-1$ is the degrees of freedom for the fit model. Fits with $\bar{R}^2 > 0.9$ are considered good fits and are used for the rest of this analysis. Figure 1a shows an example of two superposed microbursts that had a fit $\bar{R}^2 = 0.83$ that were excluded from this study. On other hand, Fig. 1b-d show microbursts that were included in this study because the fit $\bar{R}^2 > 0.9$.

Lastly, Fig. 1c,d demonstrate the necessity of the linear fit to account for the changing background. The linear fit accounts for the non-zero mean background counts and the different amplitudes of the edges of the Gaussian. Of the 256,764 detected microbursts, 110,135 had $R^2 > 0.9$ and were used for the remainder of this study.

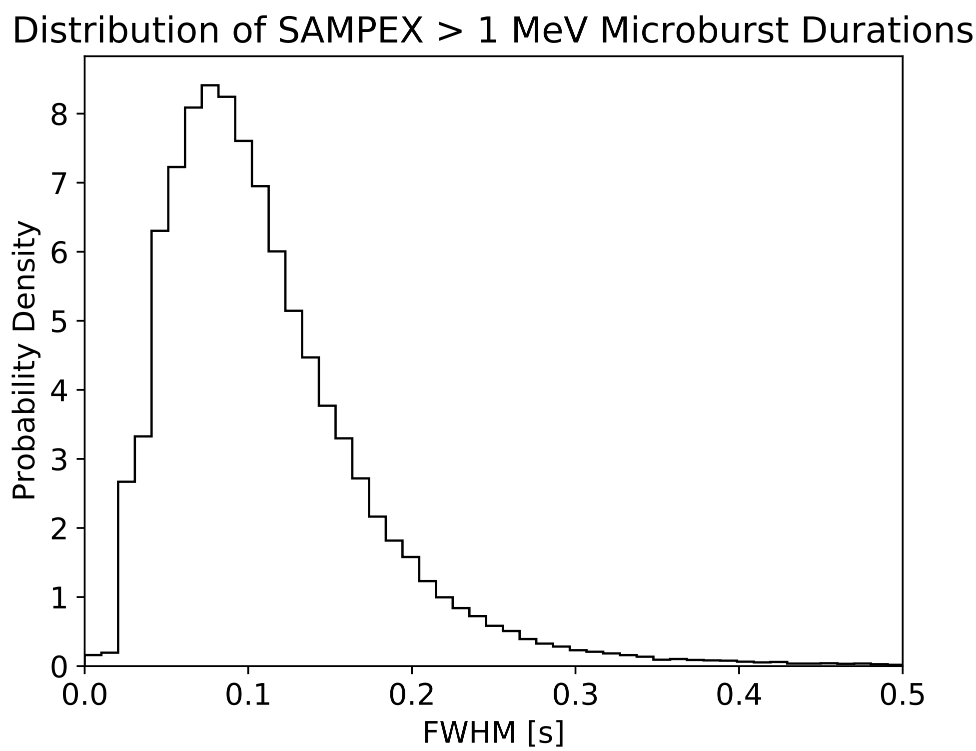

Figure 2. The distribution of all microburst full width at full maximum (FWHM).

4 Results

Outline

1. Show the entire distrubution
2. Show the L-MLT dial plots
3. Show the marginalized distribution in MLT and L shell.
4. Show the distribution with AE

5 Discussion and Conclusions

Outline

1. Compare to prior microburst width estimates.
2. Comment that microbursts at lower energy are wider (data + model). The cited microburst widths are dependent by the energy channel of the instrument.
3. Compare to chorus rising tone element duration trends.
4. A few concluding remarks.

To address the burst parameter preferential bias to narrower microbursts, as introduced in section 3.1, we ran the microburst identification algorithm on the data using three background values: A_{500}, A_{1000}, and A_{1000}. As described in section 3.1, an detection algorithm who's centered running average is over wider time periods will be more sensitive to wider and less prominent microbursts. Therefore we can identify the bias if there is a relative excess of longer duration microbursts when the average time was in-

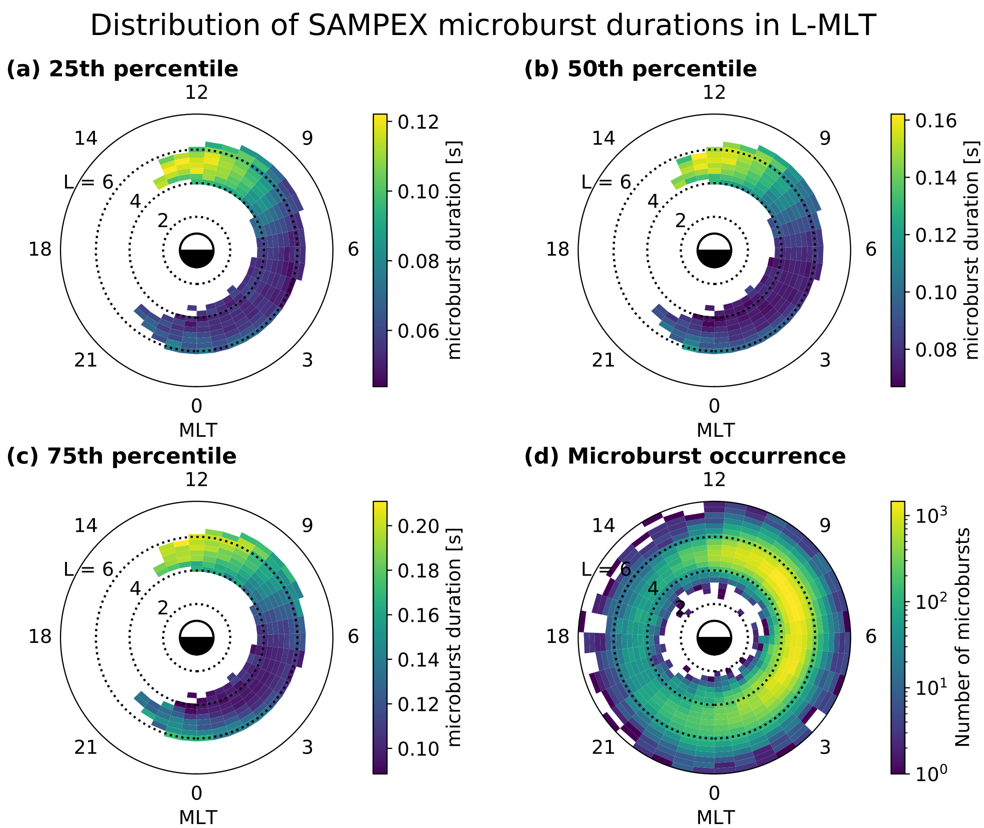

Figure 3. The joint distributions of microburst duration (FWHM) as a function of L and MLT. In each L-MLT bin with more than 100 good microburst fits, the 25th, 50th, and 75th percentiles of the duration were calculated and shown in panels a-c, respectively. The white bins in panels a-c have less than 100 good microburst fits. Panel d shows the distribution of the number of microbursts with 0 microbursts shown with the white bins.

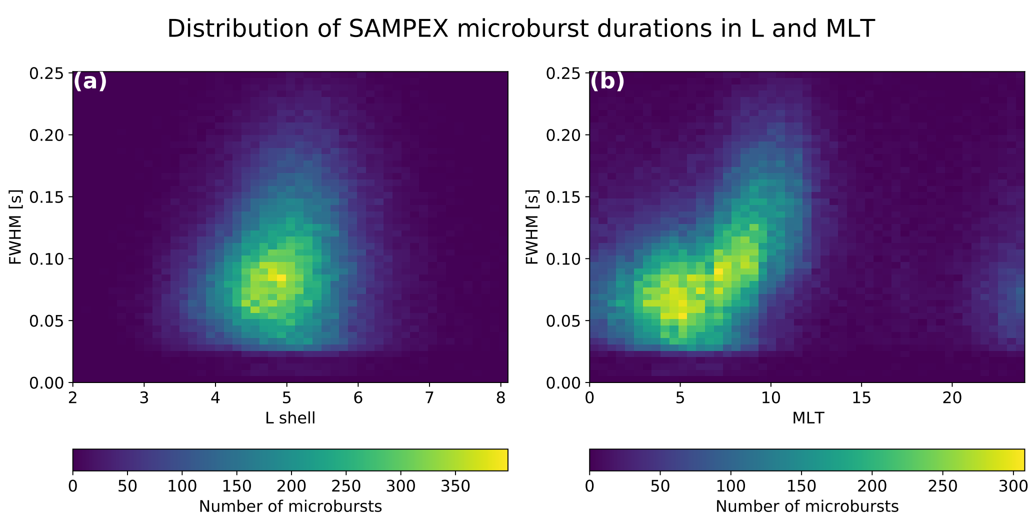

Figure 4. The marginalized distributions of the number of microbursts as a function of microburst duration (FWHM) and L shell in panel a and MLT in panel b.

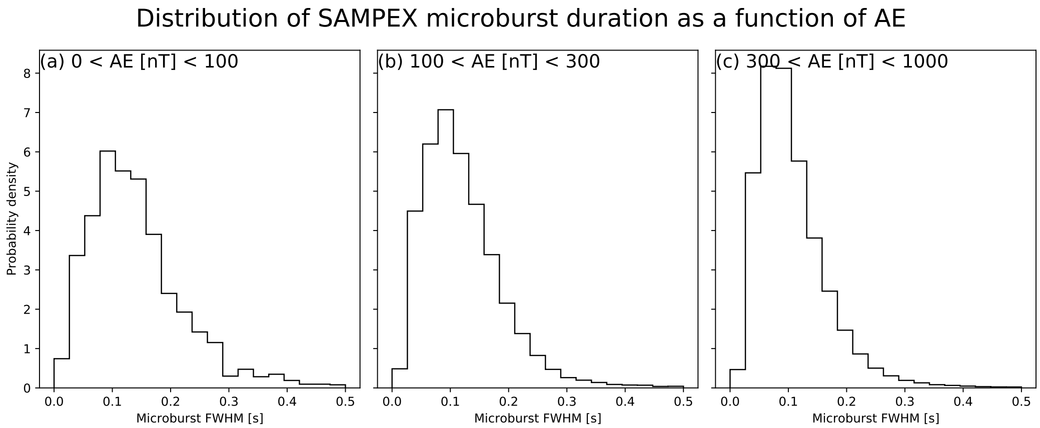

Figure 5. The distribution of the microburst duration (FWHM) for three ranges of the Auroral Electroject: AE < 100, 100 < AE < 300, and 300 < AE < 100 nT in panels a-c, respectively. The y-axis probability density shares identical limits between the three panels.

creased. We found no such excess for microburst data sets that were made using A_{1000}, and A_{1000}. Therefore, we believe that > 1 MeV microbursts are truly narrower than 250 ms and the A_{500} is adequate to identify > 1 MeV microbursts.

Acknowledgments

We are thankful for the engineers and scientists who made the SAMPEX mission possible. M. Shumko is thankful for the support provided by the NASA Postdoctoral Program at the NASA's Goddard Space Flight Center, administered by Universities Space Research Association under contract with NASA. Lauren's and Alex's funding sources The SAMPEX HILT and attitude data are located at `http://www.srl.caltech.edu/sampex/DataCenter/data.html` and the minute cadence Auroral Electroject data is located at `ftp://ftp.ngdc.noaa.gov/STP/GEOMAGNETIC_DATA/INDICES/AURORAL_ELECTROJET/ONE_MINUTE/`. The analysis software is archived at `https://github.com/mshumko/sampex_microburst_widths`.

References

Douma, E., Rodger, C. J., Blum, L. W., & Clilverd, M. A. (2017). Occurrence characteristics of relativistic electron microbursts from SAMPEX observations. *Journal of Geophysical Research: Space Physics*, *122*(8), 8096–8107. Retrieved from `http://dx.doi.org/10.1002/2017JA024067` (2017JA024067) doi: 10.1002/2017JA024067

O'Brien, T. P., Lorentzen, K. R., Mann, I. R., Meredith, N. P., Blake, J. B., Fennell, J. F., … Anderson, R. R. (2003). Energization of relativistic electrons in the presence of ULF power and MeV microbursts: Evidence for dual ULF and VLF acceleration. *Journal of Geophysical Research: Space Physics*, *108*(A8). Retrieved from `http://dx.doi.org/10.1029/2002JA009784` doi: 10.1029/2002JA009784